A Disturbance Cancellation Perspective on Vibration Control Using a Bistable Snap-Through Attachment

David R. Johnson[1]
Department of Mechanical Engineering,
University of Michigan,
Ann Arbor, MI 48109-2125
e-mail: dvdjhnsn@umich.edu

R. L. Harne
Department of Mechanical Engineering,
University of Michigan,
Ann Arbor, MI 48109-2125

K. W. Wang
Department of Mechanical Engineering,
University of Michigan,
Ann Arbor, MI 48109-2125

One approach to vibration control is to apply a force to a primary structure that opposes the excitation, effectively canceling the external disturbance. A familiar passive example of this approach is the linear-tuned mass absorber. In this spirit, the utility of a bistable attachment for attenuating vibrations, especially in terms of the high-orbit, snap-through dynamic, is investigated using the harmonic balance method and experiments. Analyses demonstrate the fundamental harmonic snap-through dynamic, having commensurate frequency with the single-frequency harmonic excitation, may generate adverse constructive forces that substantially reinforce the applied excitation, primarily at lower frequencies. However, both analyses and experiments indicate that such high-orbit dynamics may be largely destabilized by increased bistable attachment damping. Destructive forces, which substantially oppose the excitation, are unique in that they lead to a form of vibration attenuation analogous to strictly adding damping to the host structure, leaving its spectral characteristics largely unaltered. The experiments verify the analytical findings and also uncover nonlinear dynamics not predicted by the analysis, which render similar attenuation effects. [DOI: 10.1115/1.4026673]

Keywords: nonlinear vibration, vibration control, bistable, snap-through

Introduction

Structural vibration control is a well-established yet still developing field in engineering. There are a variety of ways to attenuate the vibrations of a structure via dynamic attachments to achieve damping or vibration absorption [1–4]. An emerging strategy is to use passive attachments with nonlinear characteristics in hopes of exploiting the more intricate responses to greater advantage than linear devices. Attachments with hardening stiffness nonlinearities [5,6], strategies involving mode localization with essential (nonlinearizable) stiffness nonlinearities [7,8], and targeted energy transfer from a linear structure to an attached nonlinear energy sink having an essential stiffness nonlinearity [9] have been studied extensively by experiment and analysis. Others have investigated attachments with a different type of nonlinearity—bistability—with the aim of controlling a linear structure's vibrations. It is anticipated that the energetic snap-through motions, when the inertial mass rapidly crosses the unstable equilibrium once per driving period, may be highly effective for vibration control. Bistable systems have been shown to achieve high and adaptable damping [10]. The possibility of designing nonlinear normal modes of high localized amplitude within the attached bistable truss was demonstrated [11], and these modes were shown to have stability across a relatively wide frequency range [12]. Quasiperiodic (i.e., multiharmonic) response regimes were predicted to be common for the snap-through attachment [13], and the effectiveness in attenuating transient vibrations has also been evaluated [14].

The past studies provided intent focus and interesting results on the dynamic characterization of a linear structure coupled with a bistable attachment. On the other hand, they have not assessed in detail the vibration attenuation capability of the bistable attachments in controlling the linear host structure under harmonic excitations, as compared to a baseline response without the attachment, especially in terms of the high-orbit dynamic. Furthermore, experimental demonstration has yet to be performed. To shed new light on the problem, the investigation presented in this paper evaluates the effectiveness of a bistable attachment and snap-through dynamics from the perspective that an effective attachment necessarily must provide an *opposing* or *destructive* dynamic force, i.e., an induced force that is mostly in opposition to the applied excitation. As seminally detailed by den Hartog [15] for linear vibration absorbers, the force applied to the primary structure by the attachment is "equal and opposite to the external force," leaving the primary structure "standing still". The ideal case would be an example of a *perfectly opposing* dynamic force—one that matches the applied excitation in frequency and amplitude and is exactly 180 deg out of phase. Analysis of this phenomenon reveals that the undamped linear absorber relative displacement also responds out of phase with the excitation, an anticipated result given the linear relationship between displacement and force. The addition of damping to the absorber introduces a phase shift to the reactive force such that it is not perfectly in opposition to the excitation, permitting some oscillation of the host structure at the excitation frequency but enhancing system robustness by providing modal damping [15].

The bistable oscillator has some potentially challenging characteristics when it comes to achieving opposing dynamic force, especially for the high-orbit, snap-through response. A recent study demonstrated that a directly excited bistable oscillator responds in the energetic high-orbit, snap-through dynamic only when the response displacement is in phase with the applied force. Otherwise, the high-energy, snap-through response destabilizes and the result is a low-orbit, intrawell oscillation [16]. In addition, the displacement-force curve of a bistable system is highly nonlinear and includes a region of negative stiffness. It is also well known that bistable oscillators may permit coexisting solutions, where more than one response dynamic is possible at a particular forcing frequency and amplitude. These features of a bistable

[1]Corresponding author.

Contributed by the Design Engineering Division of ASME for publication in the JOURNAL OF VIBRATION AND ACOUSTICS. Manuscript received June 25, 2013; final manuscript received January 13, 2014; published online March 27, 2014. Assoc. Editor: Philip Bayly.

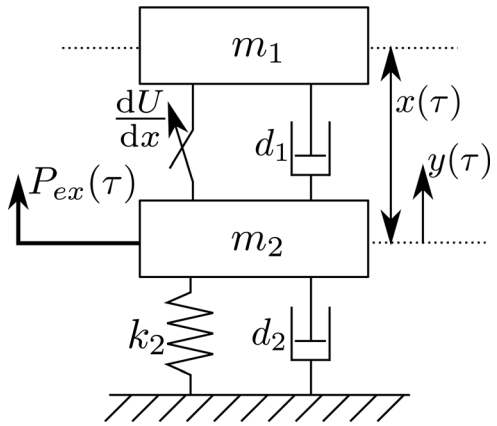

Fig. 1 Excited linear structure with bistable device attachment

attachment for the purpose of disturbance cancellation were not examined by the prior research. That is, whether destructive forces can be effectively provided by a bistable attachment for vibration suppression has not been rigorously examined and verified.

The objective of this research is to evaluate the effectiveness of an attached bistable oscillator to suppress the vibration of a linear host structure via direct cancelation of the excitation, especially in terms of the snap-through dynamic. As mentioned above, the theme is that effective vibration suppression is achieved via a destructive force applied by the bistable attachment. In contrast, a *reinforcing* or *constructive* dynamic force that acts in the same direction as the excitation would be undesirable. These are evaluated analytically first by a harmonic balance solution of a bistable oscillator attached to a harmonically excited linear host structure, a schematic of which is depicted in Fig. 1. The amplitude and phase relationships of the displacement and force produced for different designs of the attachment give insight into its performance. Experimental efforts are also carried out; test results verify the analytical findings and shed light on solution regions that are not captured by the analysis.

Analytical Formulation

In Fig. 1, a bistable attachment, denoted by subscript 1, is connected to a primary linear host structure, denoted by subscript 2, whose vibration we wish to attenuate. The motion of the bistable attachment is described by $x(\tau)$, which is the relative displacement of the bistable inertial mass with respect to the host structure mass as a deviation from the central unstable equilibrium position of the bistable attachment at $x=0$. The absolute displacement of the primary structure is described by $y(\tau)$. System parameters are prescribed as follows: m_1 and m_2 represent mass, parameters d_1 and d_2 represent damping constant, k_2 represents stiffness, $dU/dx = -k_1x + k_3x^3$ is the bistable spring force, τ is time, and overdots represent derivatives with respect to time. A periodic external force $P_{ex}(\tau) = P_o \cos\Omega\tau$ is applied to the host structure. The governing equations of motion are therefore

$$m_2\ddot{y} + d_2\dot{y} + k_2y - d_1\dot{x} + k_1x - k_3x^3 = P_o\cos\Omega\tau \tag{1a}$$

$$m_1(\ddot{x} + \ddot{y}) + d_1\dot{x} - k_1x + k_3x^3 = 0 \tag{1b}$$

We nondimensionalize and rearrange Eqs. (1*a*) and (1*b*), yielding

$$y'' + \gamma_2y' + y - \mu f\gamma_1x' + \mu f^2x - \mu f^2\beta x^3 = p\cos\omega t \tag{2a}$$

$$x'' + (1+\mu)f\gamma_1x' - (1+\mu)f^2x + (1+\mu)f^2\beta x^3 - \gamma_2y' - y = -p\cos\omega t \tag{2b}$$

where $\omega_1^2 = k_1/m_1$, $\omega_2^2 = k_2/m_2$, nondimensional time $t = \omega_2\tau$, excitation amplitude $p = P_o/k_2$, excitation frequency $\omega = \Omega/\omega_2$, mass ratio $\mu = m_1/m_2$, tuning frequency ratio $f = \omega_1/\omega_2$, nonlinearity strength $\beta = k_3/k_1$, and damping $\gamma_1 = d_1/m_1\omega_1$ and $\gamma_2 = d_2/m_2\omega_2$. Apostrophes indicate derivatives with respect to nondimensional time. The harmonic balance method is applied to solve for the responses x and y. Tseng and Dugundji [17] analytically and experimentally demonstrated that the one-term, simple harmonic motion solution provides an accurate estimation of response for a base excited bistable oscillator. Equations (3*a*) and (3*b*) therefore represent the assumed Fourier series expansion of the displacements of the bistable and linear components, respectively.

$$x(t) = c_1(t) + a_1(t)\sin\omega t + b_1(t)\cos\omega t \tag{3a}$$

$$y(t) = a_2(t)\sin\omega t + b_2(t)\cos\omega t \tag{3b}$$

The amplitude coefficients a_1, a_2, b_1, b_2, and c_1 are assumed to vary slowly. Equations (3*a*) and (3*b*) and time derivatives are substituted into Eqs. (2*a*) and (2*b*). Neglecting higher-order harmonics and equating the coefficients of constant terms $\cos\omega t$ and $\sin\omega t$, the following system of five equations for the five unknown amplitude coefficients is produced:

$$-\gamma_2a_2' + 2\omega b_2' + \mu f\gamma_1a_1' = (1-\omega^2)a_2 - \gamma_2\omega b_2 - \mu f^2\Lambda a_1 + \mu f\gamma_1\omega b_1 \tag{4a}$$

$$-2\omega a_2' - \gamma_2b_2' + \mu f\gamma_1b_1' = \gamma_2\omega a_2 + (1-\omega^2)b_2 - \mu f\gamma_1\omega a_1 - \mu f^2\Lambda b_1 - p \tag{4b}$$

$$-(1+\mu)f\gamma_1c_1' = (1+\mu)f^2\left[-1+\beta\left(c_1^2+\frac{3}{2}r_1^2\right)\right]c_1 \tag{4c}$$

$$\gamma_2a_2' - (1+\mu)f\gamma_1a_1' + 2\omega b_1' = -a_2 + \gamma_2\omega b_2 + \left[(1+\mu)f^2\Lambda - \omega^2\right]a_1 - (1+\mu)f\gamma_1\omega b_1 \tag{4d}$$

$$\gamma_2b_2' - 2\omega a_1' - (1+\mu)f\gamma_1b_1' = -\gamma_2\omega a_2 - b_2 + (1+\mu)f\gamma_1\omega a_1 + \left[(1+\mu)f^2\Lambda - \omega^2\right]b_1 + p \tag{4e}$$

where $\Lambda = -1 + \beta\left(3c_1^2 + \frac{3}{4}(a_1^2+b_1^2)\right)$. To find the steady-state values of the amplitude coefficients, we set time derivatives to zero and reduce the equation system to a single modulation equation. At steady state and after defining $r_1^2 = a_1^2 + b_1^2$ and $r_2^2 = a_2^2 + b_2^2$, Eq. (4*c*) yields

$$c_1^2 = \begin{cases} \dfrac{1}{\beta} - \dfrac{3}{2}r_1^2 \\ 0 \end{cases} \tag{5}$$

and, consequently,

$$\Lambda = \begin{cases} 2 - \dfrac{15}{4}\beta r_1^2, & c_1^2 = \dfrac{1}{\beta} - \dfrac{3}{2}r_1^2 \\ -1 + \dfrac{3}{4}\beta r_1^2, & c_1^2 = 0 \end{cases} \tag{6}$$

More explicitly, if the offset amplitude $c_1^2 \neq 0$, then oscillations occur around one of the nonzero stable equilibria, indicating low-orbit oscillations. On the other hand, if $c_1^2 = 0$, then oscillations are around the unstable equilibrium at zero relative displacement, which indicates high-orbit motion.

Equations (4*a*) and (4*b*) are solved in terms of a_2 and b_2 then substituted into Eqs. (4*d*) and (4*e*). The latter are squared and

summed to produce the following third-order polynomial for the bistable attachment relative response amplitude r_1^2:

$$p^2\omega^4 = \left\{\left[\left(f^2-(1+\mu)f^2\omega^2\right)^2+\left(f^2\gamma_2\omega\right)^2\right]\Lambda^2 + \left[-2f^2\omega^2\left\{\left(1-\omega^2\right)\left(1-(1+\mu)\omega^2\right)+(\gamma_2\omega)^2\right\}\right]\Lambda + \omega^2\left[\left(1-\omega^2\right)^2\omega^2+(f\gamma_1)^2\left(1-(1+\mu)\omega^2\right)^2 + \left((f\gamma_1\gamma_2)^2+(\gamma_2\omega)^2+2\mu f\gamma_1\gamma_2\omega^2\right)\omega^2\right]\right\}r_1^2 \equiv \alpha r_1^2 \tag{7}$$

Equation (7) can be solved for the positive, real roots of r_1^2. Using Eqs. (4*a*)–(4*d*), the amplitude coefficients are expressed in terms of Λ

$$a_1 = \frac{p\omega^3}{\alpha}\left[f^2\gamma_2\Lambda-\gamma_2\omega^2+f\gamma_1\left(1-(1+\mu)\omega^2\right)\right] \tag{8a}$$

$$b_1 = \frac{p\omega^2}{\alpha}\left[f^2\Lambda\left(1-(1+\mu)\omega^2\right)-f\gamma_1\gamma_2\omega^2-\left(1-\omega^2\right)\omega^2\right] \tag{8b}$$

$$a_2 = \frac{1}{\rho}\left[\lambda_1 a_1+\lambda_2 b_1+(\gamma_2\omega)p\right] \tag{8c}$$

$$b_2 = \frac{1}{\rho}\left[-\lambda_2 a_1+\lambda_1 b_1+\left(1-\omega^2\right)p\right] \tag{8d}$$

with terms ρ, λ_1, and λ_2 defined as

$$\rho = \left(1-\omega^2\right)^2+(\gamma_2\omega)^2 \tag{9a}$$

$$\lambda_1 = \left(1-\omega^2\right)\left(\mu f^2\Lambda\right)+(\gamma_2\omega)(\mu f\gamma_1\omega) \tag{9b}$$

$$\lambda_2 = (\gamma_2\omega)\left(\mu f^2\Lambda\right)-\left(1-\omega^2\right)(\mu f\gamma_1\omega) \tag{9c}$$

Once the amplitude coefficients have been determined, their stability must be assessed. Real and stable solutions represent physically realizable system dynamics. Stability of the solutions is determined by rewriting Eqs. (4*a*)–(4*d*) in state form and computing the eigenvalues of the Jacobian of the state matrix [18]. If all eigenvalues have negative real parts, the corresponding solution is predicted to be stable.

Equations (2*a*) and (2*b*) may be rewritten as

$$x(t) = c_1(t)+r_1(t)\cos[\omega t-\phi_1] \tag{10a}$$

$$y(t) = r_2(t)\cos[\omega t-\phi_2] \tag{10b}$$

where the phase lag of the responses behind the applied force are $\phi_1 = \tan^{-1}(a_1/b_1)$ and $\phi_2 = \tan^{-1}(a_2/b_2)$. The nondimensional force applied by the bistable attachment to the structure is

$$P_{\text{att}}(t) = \mu f\gamma_1 x' - \mu f^2 x + \mu f^2\beta x^3 \tag{11}$$

Substituting Eq. (10*a*) and its first time derivative into Eq. (11) and neglecting higher-order harmonics, we obtain

$$P_{\text{att}}(t) = P_{a1}\cos(\omega t-\Phi_1) \tag{12}$$

where the attachment force amplitude and phase are

$$P_{a1} = \mu f r_1\sqrt{(f\Lambda)^2+(\omega\gamma_1)^2} \tag{13a}$$

$$\Phi_1 = \tan^{-1}\left(\frac{f\Lambda a_1-\omega\gamma_1 b_1}{\omega\gamma_1 a_1+f\Lambda b_1}\right) \tag{13b}$$

Equation (12) can be trigonometrically summed with the excitation force applied to the host structure, $p\cos(\omega t)$, to yield the total force applied to the host structure,

$$P_{\text{tot}}(t) = A_1\cos(\omega t-\psi_1) \tag{14}$$

where the total force amplitude and phase are

$$A_1 = \sqrt{P_{a1}^2+2P_{a1}p\cos\Phi_1+p^2} \tag{15a}$$

$$\psi_1 = \tan^{-1}\left(\frac{P_{a1}\sin\Phi_1}{P_{a1}\cos\Phi_1+p}\right) \tag{15b}$$

If A_1 is close to zero, it is a consequence of the bistable attachment supplying a destructive force that substantially cancels the input.

Analytical Investigation

The displacement and force responses of the structure and bistable attachment are investigated in this section, with the goal of using these quantities to evaluate the effectiveness for attenuation of the bistable attachment and particularly for the snap-through dynamic. Figure 2 presents a study of the system response for different levels of the frequency tuning ratio f with $p=0.2$, $\mu=0.3$, $\beta=1$, and $\gamma_1=\gamma_2=0.05$. Force amplitude p and nonlinearity strength β are selected in accordance to past work [17], having validated response forms of a practical bistable buckled beam structure determined via a fundamental harmonic balance solution for such parameter values. Relatively small damping constants are set, since a small amount of damping is always present in real world systems. In all cases, the solid lines represent a snap-through response, the dashed lines represent a low-orbit response, and thin gray lines correspond to unstable dynamics. The distinction between high- and low-orbit responses is clear in the attachment response amplitude plots presented in Fig. 2(*a*). At lower frequencies, low- and high-orbit solutions coexist. In some frequency regions, it appears that no stable solution exists. Similar lack of stable solutions was evident in studies of an excited linear structure with monostable nonlinear oscillator attachment [2,19]; the conclusion drawn is that multiharmonic response would be prevalent in the bandwidths where stable solutions were absent in a fundamental harmonic investigation. The comparable lack of stable solutions for the coupled system, particularly for frequencies around $\omega=1$ in Fig. 2, encourages further examination by ensuing experiments to verify this hypothesis for the coupled system.

At a glance, Fig. 2(*c*), which represents the response amplitude of the host structure, shows that the snap-through dynamic of the bistable attachment increases the response amplitude of the primary structure over significant frequency ranges when compared to its uncoupled response—the response of the host structure without the attachment (black dotted line). This adverse influence for vibration control consistently occurs despite changing tuning ratio f, one traditional design parameter for a linear vibration absorber. As Fig. 2(*a*) shows, this region of host amplification is associated with the greatest attachment displacement amplitudes. On the other hand, in a narrow frequency region near the uncoupled resonance frequency ($\omega=1$), certain values of f, namely $f=0.5$ in Fig. 2, yield high-orbit response, which supplies some vibration suppression of the main structure. Figure 2(*a*) indicates the displacement amplitude is noticeably lower than the snap-through motion at relatively lower frequency. To explore these two regions further, the attachment force amplitude and phase according to Eq. (13) as well as the total force amplitude applied to the structure according to Eq. (15*a*) are presented in Fig. 3. Figure 3(*b*) demonstrates two distinct types of high-orbit responses. In the region below $\omega=0.85$, the force phase is mostly below 90 deg, explaining the amplification of the host structure response. In the frequency region near $\omega=1$, the force phase is mostly greater than 90 deg, lending a measure of attenuation of the host structure vibration. The magnitude of the vector sum of the applied excitation and attachment force is given in Fig. 3(*c*). This presents a clear picture of the constructive and destructive force regions produced by the attachment. Note that the displacement and force phase lag may not closely correspond as shown by comparing Figs. 2(*b*) and 3(*b*). For example, in the region of high-orbit response for $f=0.5$ just above $\omega=1$, the displacement phase

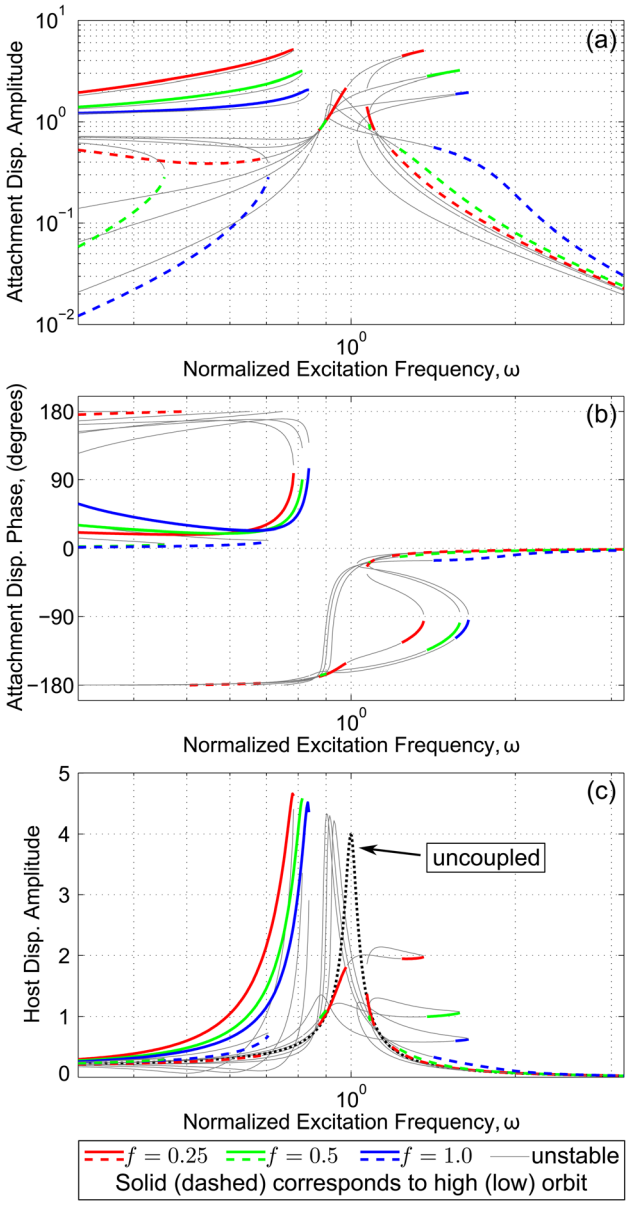

Fig. 2 System dynamics as tuning ratio *f* varies. (*a*) Bistable attachment displacement amplitude, (*b*) bistable phase lag, and (*c*) host system disp. amp.

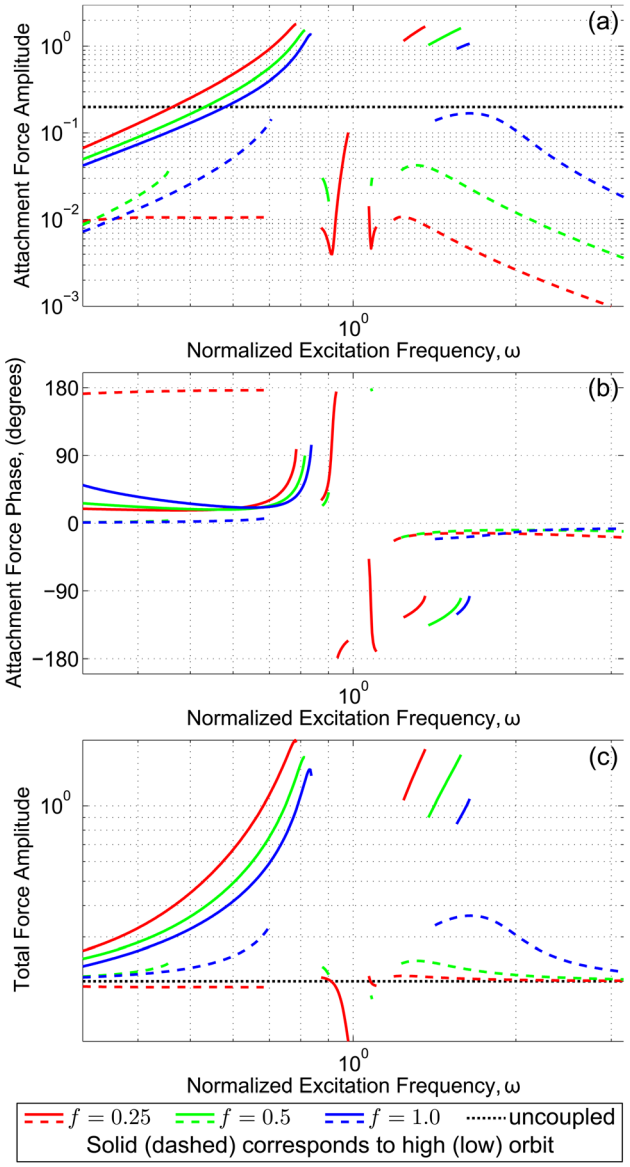

Fig. 3 (*a*) Force amplitude applied by attachment, (*b*) attachment force phase, and (*c*) total (attachment + excitation) force amplitude applied to structure for different levels of tuning ratio *f*. Unstable solutions omitted.

lag is an isolated, small segment of nearly − 30 deg (Fig. 2(*b*)) and the force phase lag is an isolated but nearly vertical segment that varies widely between about −45 deg and −170 deg (Fig. 3(*b*)).

The opposing force dynamic exhibits similar resonance characteristics and frequency as the uncoupled case as in Fig. 2(*c*) near $\omega = 1$. That is, the bistable attachment snaps through, but apart from a reduction in the primary structure response, the characteristic resonance frequency is not shifted from the original linear structure natural frequency, even though there are two distinct degrees of freedom; this phenomenon was also recently reported in Ref. [20]. Except for the break in the stability of the solution in this region, the effect on the host structure is quite similar in appearance to adding damping to the host structure, though the system actually constitutes two degrees of freedom. This is beneficial for vibration control applications, where it is difficult to enhance the damping of a primary structure while retaining its original spectral response.

Figure 4 presents a study of the response of the system for different levels of the mass ratio μ with $p = 0.2$, $f = 0.25$, $\beta = 1$, and $\gamma_1 = \gamma_2 = 0.05$. Mass ratio is varied from moderate to relatively high values ($\mu = 0.1$, 0.4, and 1.0) for the purposes of illustration, since a larger attachment is commonly able to supply a more effective reactive force. The maximum frequency of stable constructive snap-through is tailored by adjusting μ, evidenced most clearly in Fig. 4(*a*)—as mass ratio increases, the maximum stable frequency of this dynamic decreases. Near $\omega = 1$, regions of favorable destructive snap-through may exist. In this region, varying the mass ratio has a much smaller effect on the stable bandwidth of the response compared with the constructive region. Even at extremely high values of mass ratio, there is still a break in the stability of the region of destructive force near $\omega = 1$. Additionally, increasing the mass ratio causes a more effective force cancellation, as shown in Fig. 4(*b*).

Figure 5 presents a study on varying the attachment damping constant γ_1 with other parameters set to $p = 0.2$, $f = 0.25$, $\beta = 1$, $\mu = 0.3$, and $\gamma_2 = 0.05$. As the damping constant is increased, the undesirable constructive high-orbit motion becomes less stable, spanning less bandwidth for $\gamma_1 = 0.25$ than $\gamma_1 = 0.05$, and eventually vanishes, for example, due to $\gamma_1 = 0.5$. Also, as γ_1 increases,

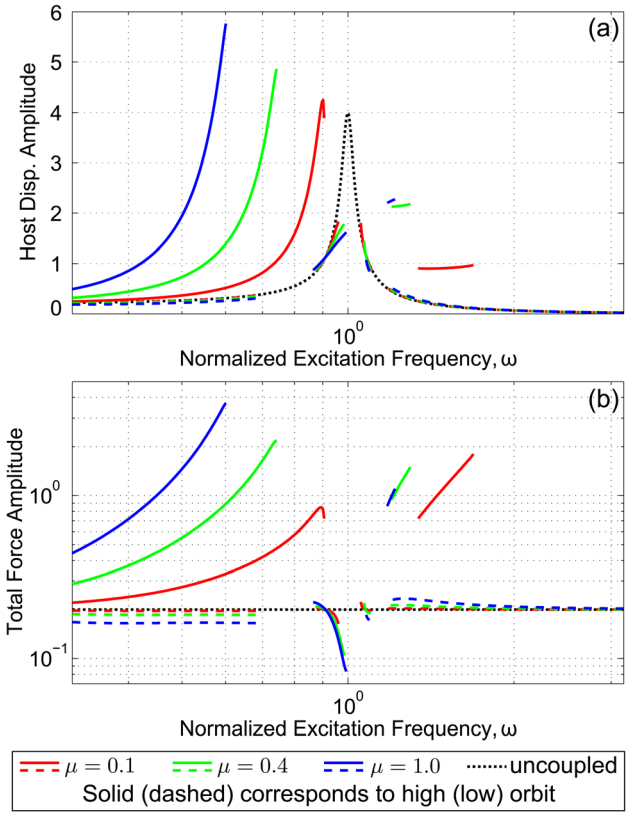

Fig. 4 System dynamics as mass ratio μ varies. (*a*) Host displacement amplitude and (*b*) total force applied to host structure. Unstable solutions omitted.

the destructive high-orbit dynamic is increasingly stabilized near the uncoupled resonance frequency, as demonstrated in the inset of Fig. 5(*a*). Adding viscous damping to a system typically shifts the phasing of the response relative to the input. In Figs. 5(*b*) and 5(*c*), as damping increases, the attachment force phase approaches 180 deg out of phase in the frequency region where the attachment force amplitude is nearly equal in magnitude to the input force, so as to maximize vibration-control effectiveness. The net effect of the forces working on the host structure is displayed in Fig. 5(*d*), where the total force applied to the host structure is minimized for increased damping constant. Loosely speaking, this is the opposite effect of increasing the damping of a linear vibration absorber, where increasing damping drives the force phase away from the ideal 180 deg out of phase at the tuned frequency of the attachment. Finally, although the attached bistable device is oscillating in high-orbit motion, its effect on the host structure is similar to simply adding damping to the host structure, as observed near $\omega = 1$ in Figs. 2(*c*), 4(*a*), and 5(*a*).

Experimental Investigation and Findings

This section seeks to experimentally validate the complex relationships predicted in the analytical investigations, notably the possibility of attenuation of host structure vibration via a destructive force. The previous section indicates that employing a bistable device as a vibration control implement is possible for some device configurations and over some frequency ranges, though it is not a straightforward task due to the variety of possible response types as well as coexisting solutions. Additionally, it is well-known that coupled nonlinear systems are more prone to induce multiharmonic responses [2,13,18,19], making a direct comparison against a linear absorber difficult if the bistable attachment diffuses the single-frequency input energy to other frequencies. Nevertheless, analysis indicates that a properly designed

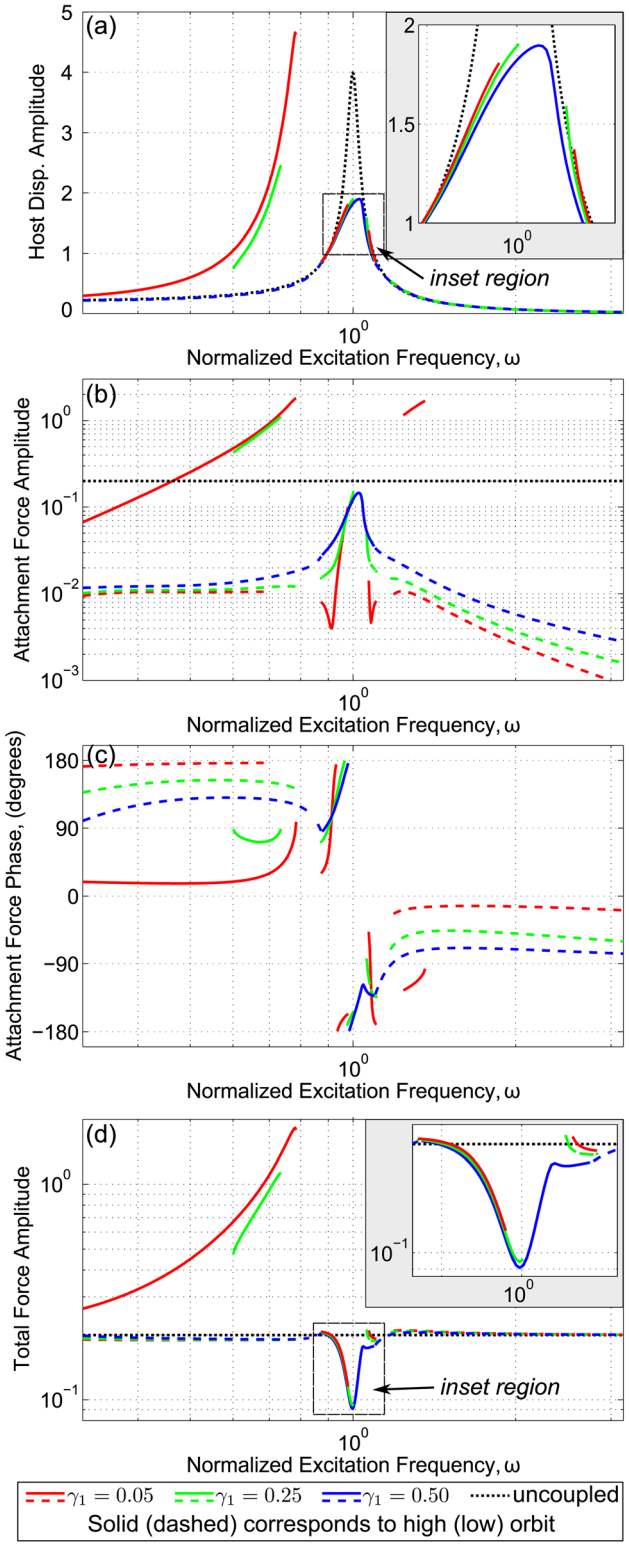

Fig. 5 System dynamics as damping constant γ_1 varies. (*a*) Host structure displacement amplitude, (*b*) attachment force amp, (*c*) attachment force phase, and (*d*) total force amp. applied to host structure. Unstable solutions omitted.

bistable attachment may be capable of high-orbit, snap-through oscillations that provide a measure of destructive force upon the primary structure near its resonance frequency. This may be accompanied by constructive snap-through forces at lower frequencies that may reinforce the excitation to the system and

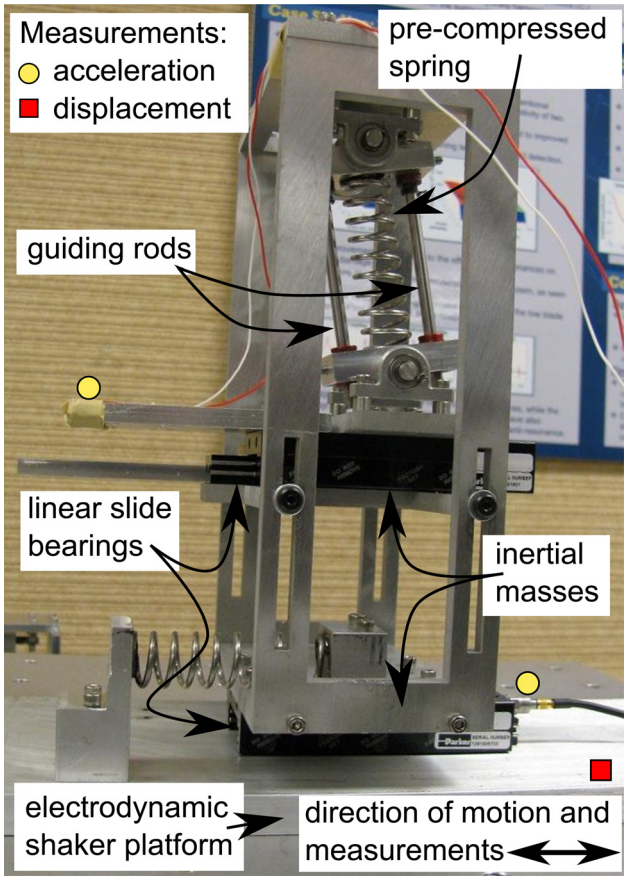

Fig. 6 Test configuration to evaluate vibration control capability of nonlinear attachments

amplify the host structure vibration, depending on system parameters.

The test configuration is shown in Fig. 6. A host linear oscillator (rectangular frame) is attached to an electrodynamic shaker platform via a low-friction translational bearing and spring. Another oscillator mass is attached to the host structure via an additional translational bearing and inclined spring. To induce a bistability for the attachment, the spring is precompressed in its upright position while guiding rods prevent twisting of the spring as the bistable device snaps through. The excitation signal to the shaker is a slowly swept sinusoid (+0.0092 Hz/second). A potentiometer measures the displacement of the shaker platform, and accelerometers measure the vibration of the oscillator inertial masses. Tests are conducted with and without the bistable attachment coupled to the host oscillator. The attachment has a mass ratio of $\mu \approx 0.39$ and tuning ratio of $f \approx 0.3$. The resonance frequency of the uncoupled linear oscillator is computed to be 5.20 Hz based on the known linear spring constant (960 N/m) and mass (0.90 kg).

Direct comparison of results between the force-excited system of the analysis and the base-excited system of the experiment is possible. Consider the governing equation for the physical system of Fig. 1, excepting that the force excitation is replaced by ground acceleration, $\ddot{z}$,

$$m_2(\ddot{v}+\ddot{z})+d_2\dot{v}+k_2v-d_1(\dot{u}-\dot{v})+k_1(u-v)-k_3(u-v)^3=0 \tag{16a}$$

$$m_1(\ddot{u}+\ddot{z})+d_1(\dot{u}-\dot{v})-k_1(u-v)+k_3(u-v)^3=0 \tag{16b}$$

Displacement coordinates are defined such that v is the displacement of the host structure and u is the displacement of the bistable attachment, both relative to the moving ground. The bistable coordinate is defined such that the inertial mass is in the unstable equilibrium position when both $u=0$ and $v=0$. Rearranging terms in Eq. (16),

$$m_2\ddot{v}+d_2\dot{v}+k_2v=-m_2\ddot{z}+\left[d_1(\dot{u}-\dot{v})-k_1(u-v)+k_3(u-v)^3\right] \tag{17a}$$

$$m_1(\ddot{u}+\ddot{z})=-\left[d_1(\dot{u}-\dot{v})-k_1(u-v)+k_3(u-v)^3\right]=-F_{\text{att}} \tag{17b}$$

Subsequently, Eq. (17*a*) becomes

$$m_2\ddot{v}+d_2\dot{v}+k_2v=-m_2\ddot{z}-m_1(\ddot{u}+\ddot{z})=F_{ex}+F_{\text{att}} \tag{18}$$

In order to compare the base-excited system with the force-excited system, we rearrange Eq. (1*b*),

$$m_1(\ddot{x}+\ddot{y})=-\left[d_1\dot{x}-k_1x+k_3x^3\right]=-P_{\text{att}} \tag{19}$$

and thereafter express Eq. (1*a*) as

$$m_2\ddot{y}+d_2\dot{y}+k_2y=P_o\cos\Omega\tau-m_1(\ddot{x}+\ddot{y})=P_{ex}+P_{\text{att}} \tag{20}$$

Equations (18) and (20) show that the force-excited system of the analysis and the base-excited system of the experiment are mathematically equivalent. The summation of excitation and bistable attachment forces (F_{ex} and F_{att}, respectively) in experimental system Eq. (18) work upon the relative vibration of the host structure v, whereas their counterpart forces (P_{ex} and P_{att}) in analytical system Eq. (20) work upon the absolute response of the host system y. Therefore, to verify the analytical development of this work, we experimentally consider system Eq. (18). Equations (18) and (20) also make clear that cancellation of input into the host system of coordinates v and y, respectively, is thus achieved when the right-hand side is zero. Note that comparing systems in Eqs. (18) and (20) indicates that following normalization of the equations, we would conclude that parameters $\omega_{1,2}$, μ, f, $\gamma_{1,2}$, and β have identical interpretations between the systems, and thus dynamical phenomena related to changes in these values from analysis likewise will have direct counterpart in the experiment.

Using the experimental data of base acceleration $\ddot{z}$ (computed from the second time derivative of the potentiometer output) and the absolute acceleration of the bistable attachment $\ddot{u}+\ddot{z}$, we may evaluate the two forces and compare their phase relationships for constructive or destructive superposition upon the host structure *relative* vibration v. This coordinate v is plotted in Fig. 7 as the acceleration frequency response function (frf) amplitude for three different levels of root-mean-square (rms) base excitation amplitude: 1.07 m/s^2 (a), 1.35 m/s^2 (b), and 1.60 m/s^2 (c). Different amplitudes are investigated since nonlinear response can change significantly depending on excitation level. The uncoupled system exhibits a strong resonance around 5.20 Hz, as predicted. For the coupled system around 2.5 to 3 Hz for each case of base acceleration, the bistable attachment snaps through with large amplitude in-phase displacements relative to the host system. Time series of the forces are plotted in Fig. 8 to verify force behavior, using a base acceleration of 1.07 m/s^2. Figure 8(*a*) shows that the bistable attachment force $F_{\text{att}}=-m_1(\ddot{u}+\ddot{z})$ is constructive with the excitation force $F_{ex}=-m_2\ddot{z}$. Note the large difference in magnitudes between the forces, the left vertical axis corresponding to the excitation and the right vertical axis corresponding to the attachment, indicating that the attachment applies a much greater force to the structure than the input force. The large constructive force explains the resulting large amplification of the host oscillator response in the frequency range around 2.5–3 Hz. This also serves to validate the analytical formulation, since it was also found that, at frequencies less than the host structure uncoupled resonance,

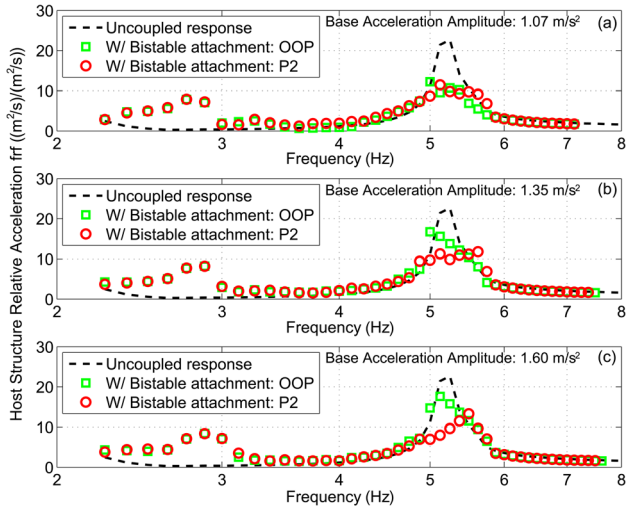

Fig. 7 Relative acceleration frf magnitude of host system with and without the bistable attachment for various base acceleration amplitudes: (*a*) 1.07 m/s^2, (*b*) 1.35 m/s^2, and (c) 1.60 m/s^2

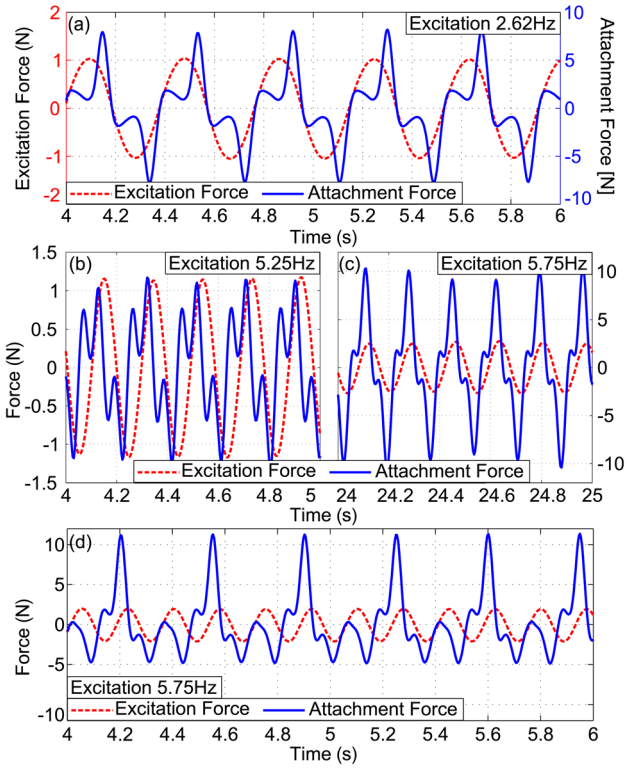

Fig. 8 Time series of forces as computed via measured data and Eq. (13). Forces plotted correspond to: (*a*) constructive snap-through at 2.62 Hz, (*b*) destructive snap-through during near-stabilization of unstable equilibrium at 5.25 Hz, (*c*) destructive snap-through at 5.75 Hz, and (*d*) P2 snap-through at 5.75 Hz.

the snap-through dynamic may provide a constructive force, leading to a large amplification in the host structure response.

Figures 2(*b*) and 2(*c*) indicate that, as forcing frequency is increased, the constructive snap-through forces may persist as the frequency approaches the uncoupled linear oscillator resonance and adversely amplify the host-system response. However, the present experimental configuration was not capable of sustaining such high-energy dynamics for frequencies greater than about 3 Hz and instead returned to small intrawell oscillations. As excitation frequency approaches 5 Hz, the coupled system is observed to undergo resonance-like behavior, during which time the bistable attachment exhibits two distinct responses, indicated in Fig. 7 as squares (out-of-phase snap-through displacements, indicated as OOP) or circles (period-2 snap-through, indicated as P2). Initial conditions determine which response form is produced, and it was experimentally observed from numerous trials that both responses appeared with near-equal probability; in fact, physical impulses into the system around these frequencies could repeatably transition the system response from P2 to OOP and back again. In the case of the coupled OOP dynamic, the unstable equilibrium position of the bistable attachment is observed to become mostly stabilized around 5–5.25 Hz. The bistable inertial mass has little motion with respect to a fixed, inertial reference frame but is still oscillating relative to the shaker base, which is the important reference frame to consider. The resulting induced attachment force is of comparable magnitude with the applied excitation. This is conducive for effective vibration cancellation, although Fig. 8(*b*) indicates that the attachment force response is partially diffused into an order-3 harmonic such that ideal out-of-phase disturbance cancellation is not obtained. Figure 7 also indicates that the primary influence for the OOP response is a damping-like effect upon the original host-structure resonance with no shift in spectral characteristics. This suggests that the bistable spring enables the attachment to behave as a purely damping device instead of like an additional degree of freedom.

As the excitation frequency increases slightly to 5.75 Hz, the bistable attachment exhibits pronounced OOP snap-through. The forces induced by the bistable attachment as shown in Fig. 8(*c*) are partially destructive with the excitation force. Approximately one-half of each excitation period in Fig. 8(*c*) indicates opposing forces, and the remaining portion of the period suggests substantial reinforcement of the excitation load. However, the trend of the OOP response plotted in Fig. 7 is in good agreement with our analytical findings in Fig. 2(*c*) for $f = 0.25$. The analyses predict that the coupled system would undergo a resonance feature in this bandwidth, which could reduce the resonance peak of the uncoupled linear system; the OOP dynamic in Fig. 7 demonstrates a similar reduction in peak amplitude as compared with the resonance peak of the uncoupled system, as the attachment force is partially destructive with the excitation. The attenuation observed near the uncoupled host-structure resonance peak during OOP snap-through is similar to the expected effect of directly adding damping to the host structure, though actually a dynamic system has been attached. This observation is in good agreement with analytical findings.

A second and repeatable dynamic leading to attenuation of host structure motion is observed near the uncoupled linear system resonance frequency. Figure 8(*d*) shows the time series of the force induced by this dynamic, during which the bistable oscillator vibrates primarily with a period-2 times that of the excitation, while the host system vibrates mostly at the driving frequency. Figure 8(*d*) indicates several moments during a forcing period when the bistable attachment and excitation forces are destructive, providing explanation for similar attenuation results as the OOP dynamic. Another explanation for this attenuation is that the net harmonic energy of the coupled system is more readily diffused from the host structure into the bistable attachment in the form of the strong period-2 harmonic. This is a similar nonlinear vibration control methodology as employed by other researchers [9], sometimes classified as "energy pumping."

Analyses predict that the snap-through dynamic that produces constructive forces may induce a dramatic amplification of the primary structural vibration over a broad band of frequencies, for example, Fig. 2(*c*), in which case the amplification could reach or exceed the amplitude of the uncoupled primary system resonance. However, we experimentally observe in Fig. 7 that this response is destabilized prior to the point at which such extreme amplification occurs. Inherent damping in the test setup could be the reason. Revisiting the analysis in Fig. 5, an increase in damping constant γ_1 leads to a decrease in the stability bandwidth and the

eventual vanishing of the constructive high-orbit dynamic. These results indicate that inherent damping in the experimental system may have suppressed the band of stability of the constructive snap-through region, providing explanation as to why the measured high-orbit responses in the 2.5–3-Hz region of Fig. 7 were destabilized prior to reaching the large peaks earlier observed in analyses, Fig. 2(*c*).

Conclusions

The effectiveness of a bistable attachment is explored by harmonic balance analysis and subsequent experiments for the purpose of supplying an opposing force to cancel disturbance and suppress the vibration of a host structure under harmonic excitation. Analysis and experiment both show that high-amplitude snap-through, which is stable at relatively low frequencies, generates forces that reinforce the excitation. Therefore, in this region, the hypothesis that energetic snap-through may be harnessed for vibration control purposes would not be valid. On the other hand, in a frequency region near the natural frequency of the original host structure, the bistable system may respond in snap-through motion and produce forces that oppose the applied excitation. The effect of the opposing force dynamic on the structure typically is similar to a direct increase of host-structure damping. As a result, the attachment effectively allows a structure to maintain its original design, in terms of spectral distribution for instance, with the appearance of enhancing the damping characteristics. The experimental investigation verifies analytical findings and also uncovers regions of period-2 oscillations in the attachment, which are also shown to suppress the amplitude of the host structure near its original (without attachment) natural frequency.

Acknowledgment

This research is partially supported by the Defense Advanced Research Projects Agency (DARPA) under Contract No. HR0011-10-C-0148, subcontracted via the Teledyne Scientific Company (TSC).

References

[1] Sun, J. Q., Jolly, M. R., and Norris, M. A., 1995, "Passive, Adaptive and Active Tuned Vibration Absorbers—A Survey," ASME J. Mech. Des., **117**(B), pp. 234–242.
[2] Tsai, M., and Wang, K. W., 1999, "On the Structural Damping Characteristics of Active Piezoelectric Actuators With Passive Shunt," J. Sound Vib., **221**(1), pp. 1–22.
[3] Morgan, R. A., and Wang, K. W., 2002, "Active–Passive Piezoelectric Absorbers for Systems Under Multiple Non-Stationary Harmonic Excitations," J. Sound Vib., **255**(4), pp. 685–700.
[4] Wang, K. W. and Tang, J., 2008, *Adaptive Structural Systems With Piezoelectric Transducer Circuitry*, Springer, New York.
[5] Shaw, J., Shaw, S. W., and Haddow, A. G., 1989, "On the Response of the Non-Linear Vibration Absorber," Int, J, Non-Linear Mech., **24**(4), pp. 281–293.
[6] Alexander, N. A., and Schilder, F., 2009, "Exploring the Performance of a Nonlinear Tuned Mass Damper," J. Sound Vib., **319**(1-2), pp. 445–462.
[7] Nayfeh, T. A., Emaci, E., and Vakakis, A. F., 1997, "Application of Nonlinear Localization to the Optimization of a Vibration Isolation System," AIAA J., **35**(8), pp. 1378–1386.
[8] Jiang, X., and Vakakis, A. F., 2003, "Dual Mode Vibration Isolation Based on Non-Linear Mode Localization," Int. J. Non-Linear Mech., **38**(6), pp. 837–850.
[9] Vakakis, A. F., Gendelman, O. V., Bergman, L. A., McFarland, D. M., Kerschen, G., and Lee, Y. S., 2008, *Nonlinear Targeted Energy Transfer in Mechanical and Structural Systems*, Springer, New York.
[10] Johnson, D. R., Thota, M., Semperlotti, F., and Wang, K. W., 2013, "On Achieving High and Adaptable Damping Via a Bistable Oscillator," Smart Mater. Struct., **22**(11), p. 115027.
[11] Avramov, K. V., and Mikhlin, Y. V., 2004, "Snap-Through Truss as a Vibration Absorber," J. Vibr. Control, **10**(2), pp. 291–308.
[12] Avramov, K. V., and Mikhlin, Y. V., 2006, "Snap-Through Truss as an Absorber of Forced Oscillations," J. Sound Vib., **290**(3-5), pp. 705–722.
[13] Avramov, K. V., and Gendelman, O. V., 2009, "Interaction of Elastic System With Snap-Through Vibration Absorber," Int. J. Non-Linear Mech., **44**(1), pp. 81–89.
[14] Gendelman, O. V., and Lamarque, C. H., 2005, "Dynamics of Linear Oscillator Coupled to Strongly Nonlinear Attachment With Multiple States of Equilibrium," Chaos, Solit. Fract., **24**(2), pp. 501–509.
[15] den Hartog, J. P., 1985, *Mechanical Vibrations*, Dover, New York.
[16] Harne, R. L., Thota, M., and Wang, K. W., 2013, "Concise and High-Fidelity Predictive Criteria for Maximizing Performance and Robustness of Bistable Energy Harvesters," Appl. Phys. Lett., **102**(5), p. 053903.
[17] Tseng, W.-Y., and Dugundji, J., 1971, "Nonlinear Vibrations of a Buckled Beam Under Harmonic Excitation," ASME J. Appl. Mech., **38**(2), pp. 467–476.
[18] Nayfeh, A. H., and Mook, D. T., 1979, *Nonlinear Oscillations*, Wiley, New York.
[19] Szemplińska-Stupnicka, W., and Bajkowski, J., 1980, "Multi-Harmonic Response in the Regions of Instability of Harmonic Solution in Multi-Degree-of-Freedom Non-Linear Systems," Int. J. Non-Linear Mech., **15**(1), pp. 1–11.
[20] Wu, Z., Harne, R. L., and Wang, K. W., 2014, "Energy Harvester Synthesis Via Coupled Linear-Bistable System With Multistable Dynamics," ASME J. Appl. Mech., **81**(6), p. 061005.